Chemistry–A European Journal
Research Article
doi.org/10.1002/chem.202303388
Chemistry Europe
European Chemical Societies Publishing
www.chemeurj.org

Hot Paper

Dehydrogenative Electrochemical Synthesis of *N*-Aryl-3,4-Dihydroquinolin-2-ones by Iodine(III)-Mediated Coupling Reaction

Jessica C. Bieniek,[a] Boris Mashtakov,[a] Dieter Schollmeyer,[a] and Siegfried R. Waldvogel*[a, b, c]

Electrochemically generated hypervalent iodine(III) species are powerful reagents for oxidative C–N coupling reactions, providing access to valuable N-heterocycles. A new electrocatalytic hypervalent iodine(III)-mediated in-cell synthesis of 1*H*-*N*-aryl-3,4-dihydroquinolin-2-ones by dehydrogenative C–N bond formation is presented. Catalytic amounts of the redox mediator, a low supporting electrolyte concentration and recycling of the solvent used make this method a sustainable alternative to electrochemical ex-cell or conventional approaches. Furthermore, inexpensive, readily available electrode materials and a simple galvanostatic set-up are applied. The broad functional group tolerance could be demonstrated by synthesizing 23 examples in yields up to 96%, with one reaction being performed on a 10-fold higher scale. Based on the obtained results a sound reaction mechanism could be proposed.

Introduction

The formation of C–N bonds represents a fundamental synthetic tool in organic chemistry, commonly used for the construction of various N-heterocycles.[1] Of particular interest is the 1*H*-3,4-dihydroquinolin-2-one scaffold since it can be found in many natural products,[2] commercial drugs,[3] and biologically active substances targeting cardiovascular,[4] autoimmune[5] and inflammatory[5,6] diseases, depression,[7,8] diabetes,[9] and Alzheimer's disease[10,11] (Figure 1).

Conventionally, the 1*H*-3,4-dihydroquinolin-2-one skeleton can be synthesized through intramolecular C–N bond formation either transition metal-catalyzed by *Buchwald-Hartwig*[12] or *Goldberg*[13] amination reactions (Scheme 1, a), or by iodine(III)-promoted transformations, applying stoichiometric amounts of the hypervalent iodine(III) species[14,15] or generating them in-situ from the corresponding iodoarenes with the aid of oxidizers (Scheme 1, b).[16–18] Despite the broad applicability of the above-mentioned syntheses, they suffer from disadvantages in terms of sustainability, safety and cost efficiency. Often pre-functionalized substrates, expensive transition metal catalysts, and stoichiometric amounts of highly reactive oxidizers are required. This leads to a large amount of reagent waste, a poor atom economy, high costs and safety hazards.

Electro-organic synthesis offers a highly sustainable, inexpensive and inherently safe alternative to conventional synthesis methods, as it uses electric current as a traceless oxidant, replacing hazardous redox agents and decreasing the amount of reagent waste.[19–23] Moreover, the conversion can be easily controlled by regulation of current density and applied charge, allowing precise reaction control and an easy scale-up.[20] This makes electro-organic synthesis a broadly applicable and "green" technology, which enables chemical transformations with an improved ecological footprint.[19–21,23]

In the recent years, many efforts have been made to combine the advantages of electrosynthesis and the tremendous synthetic power of hypervalent iodine(III) species[15,18,24,25] by generating them in-situ using electric current as oxidizing agent.[26–33] Due to the elevated oxidation potentials of iodoar-

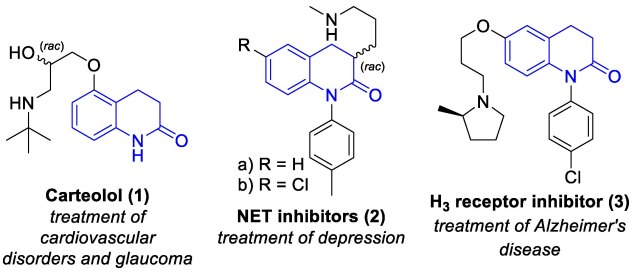

Figure 1. Biologically active compounds containing a 1*H*-3,4-dihydroquinolin-2-one scaffold.[3,7,10] NET = Norepinephrine transporter. H_3 = Histamine H_3.

[a] J. C. Bieniek, B. Mashtakov, Dr. D. Schollmeyer, Prof. Dr. S. R. Waldvogel
Department of Chemistry
Johannes Gutenberg University Mainz
Duesbergweg 10–14, 55128 Mainz (Germany)
E-mail: waldvogel@uni-mainz.de
Homepage: http://www.aksw.uni-mainz.de/

[b] Prof. Dr. S. R. Waldvogel
Institute of Biological and Chemical Systems – Functional Molecular Systems (IBCS-FMS)
Kaiserstraße 12, 76131 Karlsruhe (Germany)

[c] Prof. Dr. S. R. Waldvogel
Max-Planck-Institute for Chemical Energy Conversion
Stiftstraße 34–36, 45470 Mülheim an der Ruhr (Germany)

Supporting information for this article is available on the WWW under https://doi.org/10.1002/chem.202303388

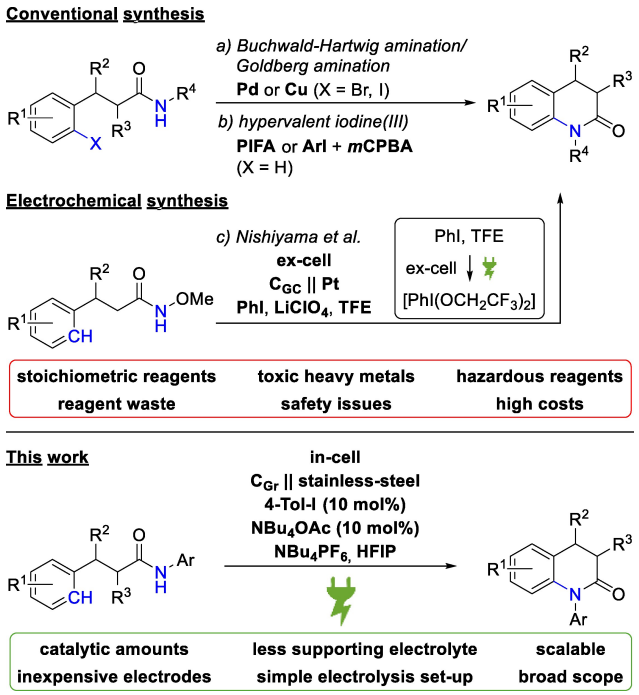

Scheme 1. Conventional and electrochemical approaches for the synthesis of the 1*H*-3,4-dihydroquinolin-2-one scaffold. PIFA = Bis(trifluoroacetoxy)-iodobenzene, ArI = aryl iodide, *m*CPBA = *meta*-chloroperoxybenzoic acid, TFE = 2,2,2-trifluoroethanol, 4-Tol-I = 4-iodotoluene, HFIP = 1,1,1,3,3,3-hexafluoro-2-propanol.

enes, often only ex-cell approaches can be implemented, in which the iodoarene is first completely converted anodically to the corresponding hypervalent iodine(III) species, followed by addition of the substrate.[26–29] An electrochemical hypervalent iodine(III)-mediated ex-cell synthesis of 1*H*-3,4-dihydroquinolin-2-ones was reported by the *Nishiyama* lab (Scheme 1, c).[34,35] They electrolyzed two equivalents of iodobenzene with $LiClO_4$ in 2,2,2-trifluoroethanol under constant current conditions applying a glassy carbon anode and a platinum cathode, followed by addition of the *N*-methoxy-3-arylpropanamide substrate.[34] Although this method provided higher product yields than when PIFA was used, the advantages of electrosynthesis are partially circumvented in this ex-cell approach, since stoichiometric amounts of iodobenzene are required.[26] Furthermore, the use of $LiClO_4$ in combination with organic compounds involves an explosion risk, which makes scale-up difficult. Additionally, expensive, and limited platinum was used as electrode material, and only few *N*-methoxy-substituted derivatives were accessible by this method, limiting the applicability of the reaction.

Electrochemical in-cell syntheses to prepare the similar phenanthridin-6-one scaffold by C–N coupling have been published, for example, by the *Waldvogel* group,[36] and by *Zhang, Xu, Zeng et al.*,[37] who were further able to apply their protocol to synthesize one single quinolin-2-one example. However, no broadly applicable electrochemical in-cell approach for the synthesis of the 3,4-dihydroquinolin-2-one scaffold by C–N coupling is known yet.

Previous reports of the *Waldvogel* lab demonstrate that the anodic oxidation of amide precursors is a powerful tool for various N–X coupling reactions.[36,38–40] Based on this knowledge, a new electrocatalytic hypervalent iodine(III)-mediated in-cell synthesis of 1*H*-*N*-aryl-3,4-dihydroquinolin-2-ones by a dehydrogenative C-N coupling reaction has been developed. This method features a broad scope and excellent scalability, applying a simple reaction set-up, inexpensive electrode materials and a low supporting electrolyte concentration.

Results and Discussion

The optimization of the reaction conditions (see Supporting Information for detailed information) was conducted with the easily accessible hydrocinnamamide **4a** as test substrate. First, **4a** was electrolyzed under constant current conditions in an undivided 5 mL Teflon™ cell,[41] applying a graphite anode and a platinum cathode, NBu_4PF_6 as supporting electrolyte and 1,1,1,3,3,3-hexafluoro-2-propanol (HFIP) as solvent. Under these conditions the desired product **5a** could be obtained in 12% HPLC-yield (Table 1, Entry 1). Performing the reaction under quasi-divided[42] conditions by using a platinum wire as cathode gave similar results (Table 1, Entry 2). The product yield increased significantly when catalytic amounts of 4-iodotoluene (4-Tol-I) in combination with NBu_4OAc as ligand donor were used as redox mediator to form a hypervalent iodine(III) species in-situ (Table 1, Entry 3). This combination was superior to the other tested iodoarenes and ligands in terms of product yield, sustainability, and costs (see Supporting Information). Substituting NBu_4PF_6 by an equimolar amount of NBu_4OAc resulted in a

Table 1. Optimization of reaction conditions for the synthesis of **5a**.[a]

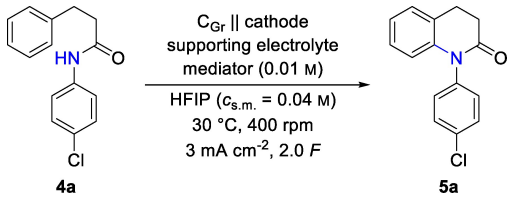

Entry	Cathode	Supporting electrolyte	Mediator	**5a**[b] (%)	**4a**[b,c] (%)
1	Pt	NBu_4PF_6 (0.01 M)	–	12	43
2	Pt wire[d]	NBu_4PF_6 (0.01 M)	–	15	40
3	Pt	NBu_4PF_6 (0.01 M), NBu_4OAc (0.02 M)	4-Tol-I	53	16
4	Pt	NBu_4OAc (0.03 M)	4-Tol-I	23	25
5	stainless-steel	NBu_4PF_6 (0.01 M), NBu_4OAc (0.02 M)	4-Tol-I	51	10
6	C_{Gr}	NBu_4PF_6 (0.01 M), NBu_4OAc (0.02 M)	4-Tol-I	46	27

[a] Substrate **4a** (0.2 mmol), HFIP (5 mL), undivided 5 mL Teflon™ screening cell. C_{Gr} = isostatic graphite. HFIP = 1,1,1,3,3,3-hexafluoro-2-propanol. 4-Tol-I = 4-iodotoluene. [b] Yield determined by HPLC calibration of the UV signal at 254 nm, using 2-naphthol as internal standard. [c] Residual starting material (s.m.) **4a**. [d] Quasi-divided set-up realized by using a Pt wire as cathode.

yield drop of **5a** (Table 1, Entry 4), indicating that NBu_4PF_6 plays a crucial role for successful product formation. The solvent screening revealed that only HFIP provides the desired product in significant amounts, which might be explained with the unique solvation properties of HFIP, being able to stabilize intermediates efficiently through strong H-bond formation.[43] To ensure a sustainable reaction performance, the HFIP used was recovered by distillation and recycled to be further used for electrolysis reactions. Among the tested anode materials, isostatic graphite led to the highest product yields (see Supporting Information). When screening cathode materials, stainless-steel and isostatic graphite as inexpensive and readily available materials proved to be an alternative to platinum, providing **5a** in comparable amounts (Table 1, Entry 5–6). Since isostatic graphite showed higher amounts of residual starting material **4a**, it was most promising regarding the theoretically accessible product yield and was therefore used as cathode material in the subsequent optimization of the following continuous parameters: amounts of the starting material **4a**, NBu_4PF_6, 4-Tol-I and NBu_4OAc, temperature, stirring speed, current density, and applied charge. The optimization of the continuous parameters was performed applying the statistics-based method *Design of Experiments* (*DoE*), which allows the simultaneous screening of multiple parameters and has proven to be very efficient for the optimization of reaction conditions.[44] Evaluating the performed *DoE* experiments revealed that the concentration of starting material (s.m.) **4a** could be increased to $c_{s.m.} = 0.06$ M, while the amounts of 4-Tol-I and NBu_4OAc could be lowered to 10 mol%, based on **4a**, without any significant negative impact on the reaction. Low current densities turned out to be beneficial for the reaction, which is why a current density of 1 mA cm^{-2} was chosen. Yield maxima for product **5a** were found at a NBu_4PF_6 concentration of 0.01 M, a reaction temperature of 40 °C, and a stirring speed of 400 rotations per minute (rpm). Regarding the applied charge, product formation increased significantly with increasing applied charge between 1.0 *F* and 2.0 *F*, whereas it remained unaffected in the range from 3.0 *F* to 4.5 *F*, despite ongoing consumption of substrate **4a**. To further determine the optimum of the applied charge, a linear screening in the range between 2.0 *F* and 3.3 *F* was performed afterwards, applying the through *DoE* identified optimal conditions for the other parameters (Figure 2). The linear screening of the applied charge revealed that the product yield reached a maximum of 66% at 3.0 *F* and remained constant at higher values of the applied charge (Figure 2, blue graphs). Despite continuous consumption of substrate **4a** no complete conversion could be achieved in the range up to 3.3 *F*, which is why a quasi-divided set-up was applied to suppress possible side reactions at the cathode. For this, various rod-shaped cathodes of different materials with a small surface area were tested (see Supporting Information). A quasi-divided set-up with a stainless-steel wire as cathode led to the best results, with which a yield maximum of 74% at almost full conversion could be achieved with an applied charge of 2.4 *F* (Figure 2, orange graphs). At higher values of the applied charge the product yield decreased, indicating a decomposition of the product. This is in line with

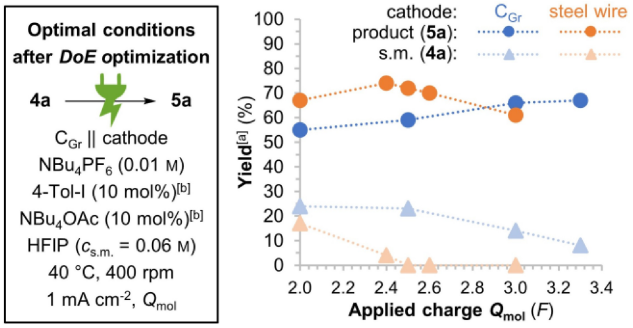

Figure 2. Influence of the applied charge on the yield of **5a** and residual starting material (s.m.) **4a**, using an undivided set-up with an isostatic graphite cathode (blue curves) and a quasi-divided set-up with a stainless-steel wire as cathode (orange curves). [a] Yield determined by HPLC calibration of the UV signal at 254 nm, using 2-naphthol as internal standard. [b] Based on the amount of starting material **4a**.

the performed cyclic voltammetry (CV) measurements, which proved a possible overoxidation of the product (see Supporting Information for details). To evaluate whether the quasi-divided set-up or stainless-steel as cathode material had a greater impact on the reaction, the reaction was further tested under the same conditions with 2.4 *F* in an undivided set-up, employing a stainless-steel cathode. This resulted in a similar product yield of 73%, which is why stainless-steel was further used as the cathode material, and both set-ups (undivided and quasi-divided) were applied when investigating the scope of the reaction (see Supporting Information).

With these optimized reaction conditions in hand first various substrates with various anilide moieties were examined (Scheme 2). The test derivative **5a** could be isolated in 69%

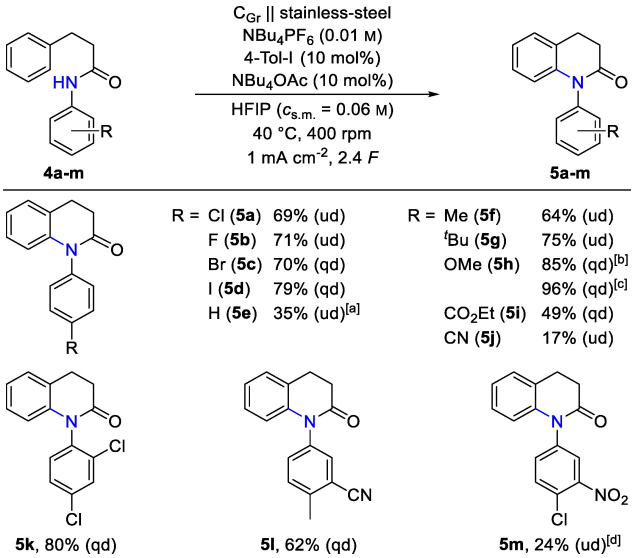

Scheme 2. Reaction scope with different anilide substituents. Undivided 5 mL Teflon™ screening cell, substrate (0.3 mmol), HFIP (5 mL), stainless-steel cathode for undivided (ud) set-up, stainless-steel wire for quasi-divided (qd) set-up. Isolated yields are provided for the set-up with the best results. NMR-yields for other tested set-ups and conditions are given in the Supporting Information. [a] 4-Tol-I (20 mol%), NBu_4OAc (20 mol%), 2.8 *F*. [b] 4-Tol-I (5 mol%), NBu_4OAc (5 mol%). [c] Without 4-Tol-I and NBu_4OAc. [d] 4-Tol-I (5 mol%), NBu_4OAc (5 mol%), 3.5 *F*.

yield after electrolysis under undivided conditions. All the other *p*-halogen-substituted derivatives **5b–d** were obtained in similar yields up to 79%, with substrates **4c** and **4d** being electrolyzed under quasi-divided conditions. This demonstrates that under the stated conditions both the electron-deficient fluoro as well as the redox-sensitive iodo substituent are perfectly tolerated in the reaction. The disubstituted derivative **5k** with two chloro substituents in *o*- and *p*-position could be isolated in a high yield of 80%. In contrast, derivative **5e** without any substituent at the aniline ring was obtained in a moderate yield of 35%, which can be explained by possible side reactions at the *p*-position of the aniline ring and is in accordance with previous observations.[38,39] Substrates without an aromatic moiety at the amide-nitrogen, but with a primary amide or a secondary ^{t}Bu-substituted amide failed to provide the corresponding 1*H*-3,4-dihydroquinolin-2-ones. This proves that an aromatic ring attached to the amide group is necessary for successful product formation as it stabilizes the formed amidyl intermediates. When investigating substrates with alkyl-substituted anilide moieties, **4f** with a *p*-methyl group and thus bearing an unprotected benzylic position could be converted successfully with a good yield of 64% into compound **5f**, which represents the core motif of NET inhibitor **2a** (Figure 1). The yield for the ^{t}Bu-substituted derivative **5g** without an unprotected benzylic position was even higher with 75%. Examination of substrate **4h** bearing a strong electron-donating *p*-methoxy group showed that the yield of **5h** increased significantly with decreasing mediator loading (see Supporting Information). With only 5 mol% of the mediator product **5h** could be obtained in a very good yield of 85% under quasi-divided conditions. Since oxidation potentials of highly electron-rich compounds are shifted towards less positive values,[39,45] it was assumed that the oxidation of substrate **4h** might occur prior to the oxidation of 4-Tol-I, which would no longer result in a mediated reaction. This was confirmed by CV measurements, showing a much lower oxidation potential for **4h** ($E_{p/2} = 1.14$ V) than for the mediator system consisting of 4-Tol-I and NBu_4OAc ($E_{p/2} = 1.60$ V). Therefore, substrate **4h** was tested in a direct electrolysis applying only NBu_4PF_6 as supporting electrolyte in HFIP, without using 4-Tol-I and NBu_4OAc, which provided the desired product **5h** in an excellent yield of 96%. These results demonstrate that substrates with an enhanced electron density at the anilide moiety are beneficial for the reaction and yield the desired 1*H*-3,4-dihydroquinolin-2-ones selectively in high yields even under direct electrolysis conditions. Regarding electron-deficient substrates, compound **5i** with a *p*-ester group was obtained in 49% yield, while a *p*-cyano substituent resulted in a poor yield of 17% for **5j**. However, when placing the electron-withdrawing cyano group in *m*-position, combined with a *p*-methyl substituent, the corresponding product **5l** was obtained in similar yield to that of the *p*-methyl-substituted derivative **5f**, regardless of whether an undivided or quasi-divided set-up was used (see Supporting Information). Finally, substrate **4m** with a redox-sensitive nitro-group in *m*-position could be converted into the desired product in 24% yield under undivided conditions, confirming the broad applicability of the herein presented method.

In the next step, substrates based on various 3-aryl propionic acids were investigated (Scheme 3). Substrates **4n–p** with substituents at the propyl chain yielded the corresponding 3,4-substituted 1*H*-3,4-dihydroquinolin-2-ones **5n–p** in 47–86%. It's particularly noticeable, that acetyl protected amino and hydroxy groups were tolerated in the reaction, affording the products **5n** and **5o** in yields up to 54%. Substrate **4n** was employed as racemic mixture, while substrate **4o** was used as enantiopure substance, yielding the enantiopure product **5o**. This demonstrates that the stereo configuration is conserved during the reaction. The racemic substrate **4p** could be converted into racemic product **5p** in a very good yield of 86% under quasi-divided conditions at a 0.3 mmol scale as well as at a 10-fold larger scale. This confirms the excellent scalability of the reaction.

Afterwards, various substrates with a R^1 substituent at the core aryl ring *meta* to the propyl chain were examined. Compound **5q**, which represents the core motif of NET inhibitor **2b** (Figure 1) bearing a *m*-chloro substituent, was formed as main product in 54% yield, applying quasi-divided conditions. Substrate **4r** with a *m*-iodo substituent yielded product **5r** in similar amounts. Interestingly, traces of three additionally formed regioisomers with the iodo substituent located at the 5-, 7- or 8-position of the 1*H*-3,4-dihydroquinoline-2-one scaffold were observed. When testing an electron-withdrawing *m*-fluoro substituent, the expected derivative **5s** was isolated in 51% yield as major product, despite the decreased electron density at the position of the newly formed C-N bond. Regioisomer **5s'** was obtained in 16% yield as minor product. Conversely, an electron-donating *m*-methoxy group led to the formation of a complex product mixture, whereby the desired product could not be isolated. With a less electron-donating methyl substituent in *m*-position the expected product **5u** was obtained in a poor yield. However, additionally regioisomer **5u''** was formed in comparable amounts, and regioisomer **5u'** was isolated as the major product in 32% yield. This indicates that substrates with electron-donating *m*-substituents on the core aryl ring are poorly suitable for the reaction. Nevertheless, motifs with a hydroxy based substituent in 6-position of the 1*H*-3,4-dihydroquinolin-2-one scaffold, as it can be found in the histamine H_3 receptor inhibitor **3** (Figure 1), are still accessible with the herein described method. This could be demonstrated with substrate **4t** bearing a pivaloyl-protected hydroxy group in *m*-position, being converted to derivative **5t** in 42% yield.

Next, substrates with a R^1 substituent *para* to the propyl chain were investigated. Substrate **4v** didn't yield the expected product when being electrolyzed with 5 mol% of the mediator but was selectively converted with 75% yield into compound **5v**, with the bromo substituent shifted one position relative to starting material **4v**. The same behavior was observed with substrate **4w** bearing an ester group in *p*-position, whereas the lower yield might be explained with the unprotected *p*-position of the aniline ring. Substrates with electron-donating substituents in *p*-position and the possibility to eliminate a leaving group, such as a *p*-methoxy or *p*-methyl substituent, provided

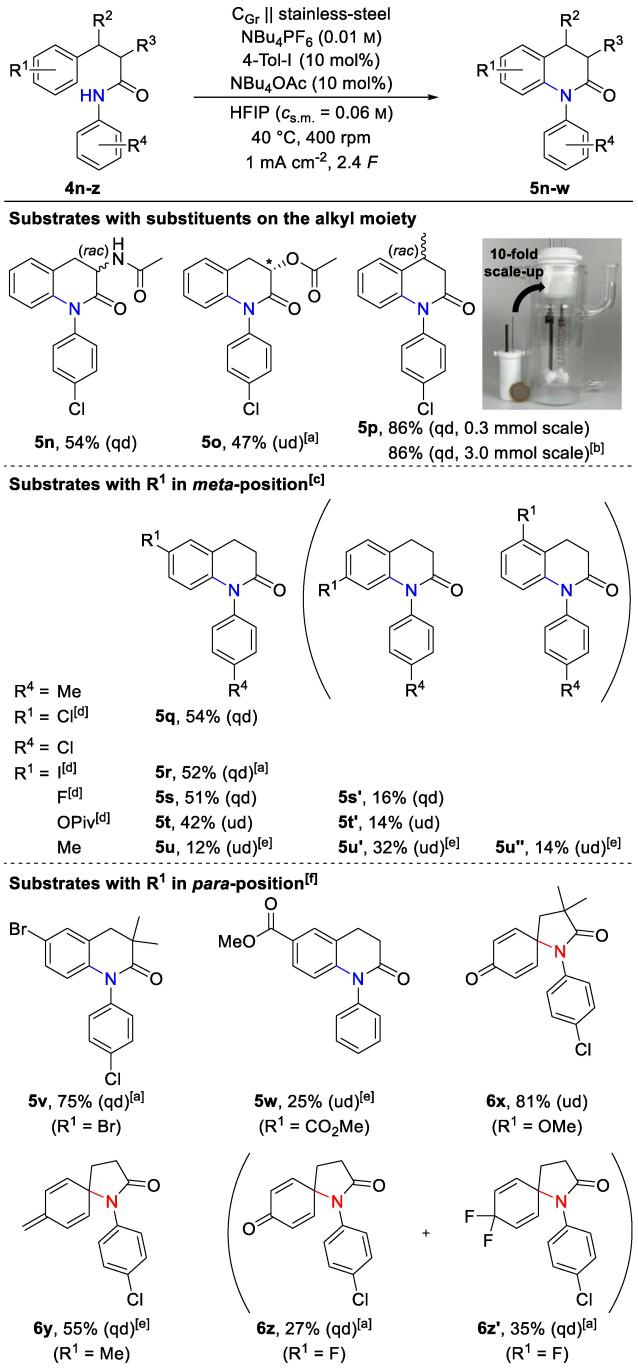

Scheme 3. Reaction scope based on different 3-aryl propionic amides. Undivided 5 mL Teflon™ screening cell, substrate (0.3 mmol), HFIP (5 mL), stainless-steel cathode for undivided (ud) set-up, stainless-steel wire for quasi-divided (qd) set-up. Isolated yields are provided for the set-up with the best results. NMR yields for other tested set-ups and conditions are given in the Supporting Information. [a] 4-Tol-I (5 mol%), NBu_4OAc (5 mol%). [b] 60 mL glass cell (illustrated in relation to a 5 mL Teflon™ screening cell and 1 € coin), substrate (3.0 mmol), HFIP (50 mL). [c] Regioisomer with R^1 in 8-position of the 1*H*-3,4-dihydroquinolin-2-one scaffold is only formed in traces and not depicted. [d] The other depicted regioisomers are formed in traces. [e] 4-Tol-I (20 mol%), NBu_4OAc (20 mol%). [f] Spirolactams **6x–z'** are formed applying the above shown reaction conditions from substrates **4x–z**.

spirolactams **6x** and **6y**[46] selectively with no formation of the desired 1*H*-3,4-dihydroquinolin-2-ones, which is in line with previous reports.[14,16,24,47] This is a common pathway in oxidative coupling reactions.[48] Substrate **4z** with a *p*-fluoro substituent yielded spirolactams **6z** and **6z'**[46] in similar amounts. This might be explained by a nucleophilic substitution of the fluoro substituent with a hydroxy species, followed by a transfer of the fluoride to another substrate. In summary, these results indicate that substrates with a *p*-substitution at the core aryl ring undergo spiro-cyclization with either subsequent rearrangement to the corresponding 1*H*-3,4-dihydroquinolin-2-ones or with formation of a spirolactam, depending on the type of substituent.

To get insights into the reaction mechanism, CV measurements of the substrates and the mediator system, consisting of 4-Tol-I and NBu_4OAc, were performed, and half peak potentials for the first oxidation wave were determined (see Supporting Information for details). The data revealed that the anilide moiety is the electrophore of the substrates and thus defines their oxidation potential. An exception is substrate **4x**, which is oxidized at the anisole moiety prior to the anilide. The substrates were sorted into three groups, depending on their oxidation potential relative to the mediator, which correlates with the electron density at the anilide moiety. The grouping is illustrated in Scheme 4, top. For each group, a different mechanism is proposed (Scheme 4). More detailed explanations are provided in the Supporting Information. Substrates with an electron-deficient anilide moiety are oxidized at higher potentials than the mediator. It can be assumed that for this group the mechanism proceeds via the hypervalent iodine(III) species **7**, which is generated at the anode from 4-Tol-I.[26,33] Then, substrate $\mathbf{4}^{D}$ reacts with species **7**, leading to intermediate **I**. Attack by the π electrons of the core aryl ring, which can happen through an electron pair (cationic pathway) or a single electron (radical pathway), and elimination of the mediator leads to product $\mathbf{5}^{D}$. This mechanism is supported by the literature.[16,26] The second group are electron-rich substrates, represented by **4h**. The oxidation potential of **4h** is strongly shifted towards less positive potentials compared to the mediator, and high yields of **5h** can be achieved in absence of the mediator. Therefore, a direct oxidation mechanism for substrate **4h** is proposed, where a two-fold oxidation at the anode leads to cationic intermediate **II**, which is attacked by the π system and yields **5h** after deprotonation. Substrates of the third group bear anilide moieties with a medium electron density. Their oxidation potentials are similar or only slightly lower than the one of the mediator. Therefore, different mechanistic pathways are conceivable for this group, which can coexist (Scheme 4, bottom). Substrate $\mathbf{4}^{M}$ can either be directly oxidized at the anode, or 4-Tol-I is oxidized at the anode to form radical species **8**, which then oxidizes $\mathbf{4}^{M}$ through a single electron transfer process. In both cases amidyl radical **III** is formed. Intermediate **III** can then be attacked by the π electrons of the core arene, and oxidized again at the anode, yielding $\mathbf{5}^{M}$ through a direct pathway, without involving the mediator. Alternatively, amidyl radical **III** can react with 4-Tol-I to form intermediate **IV**, which is either oxidized to species **V**, or attacked radically by the π system, to form product $\mathbf{5}^{M}$ after elimination of 4-Tol-I and subsequent oxidation. If species **V** is

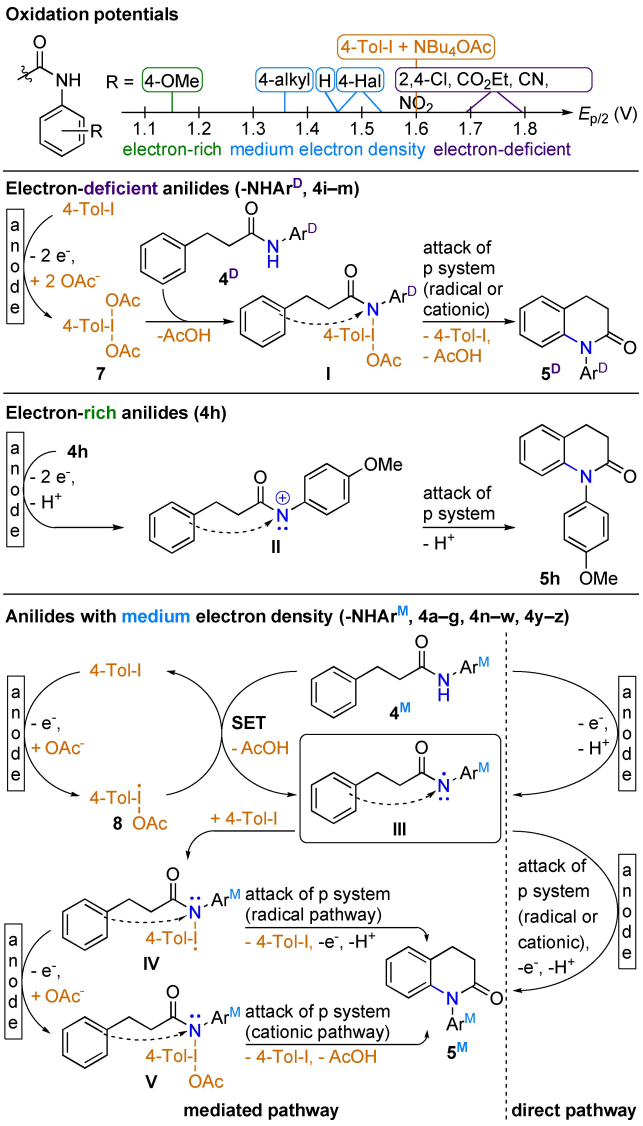

Scheme 4. Grouping of the substrates according to their oxidation potential (top) and proposed mechanisms for each group (center, bottom). SET = single electron transfer.

formed, the attack of an electron pair from the π system and elimination of 4-Tol-I lead to **5M**. Due to the limited analytical methods it's not possible to make a definite statement about which of the proposed mechanisms takes place predominantly. However, when substrates **4f** and **4g**, which exhibit lower oxidation potentials than the mediator, were employed in a direct electrolysis without mediator, product yields dropped significantly (see Supporting Information). This indicates that the mediator seems to play a crucial role for improved reaction performance, making a mediated pathway likely.

Different 3,4-dihydroquinolin-2-one regioisomers were obtained for substrates **4q–u**, bearing a *m*-substituent on the core arene. The position of the newly established C–N bond depends on whether the formed amidyl radical **VI** is attacked by the π system through pathway **a)**, **b)** or **c)** (Scheme 5). Pathways **a)** and **b)** lead directly to 3,4-dihydroquinolin-2-one intermediates

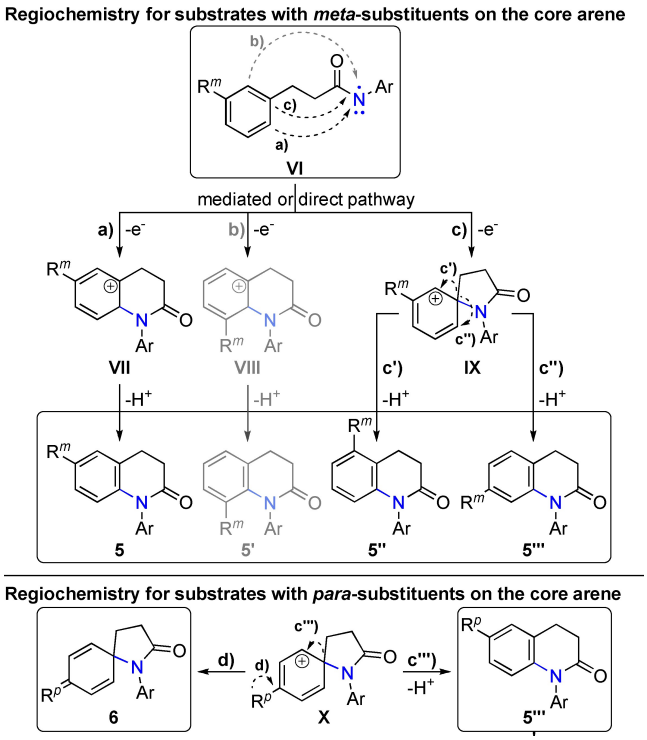

Scheme 5. Regiochemistry for substrates with *meta*- and *para*-substituents on the core arene.

VII and **VIII**, involving a second oxidation step. Deprotonation yields products **5** and **5′**. Based on the results obtained when investigating the scope, it can be assumed that pathway **b)** is less likely than the other ones, since regioisomer **5′** was formed only in traces for all tested substrates. This might be explained by the steric hindrance caused by the R^m substituent. The third possible pathway is **c)**, where spiro-cyclization and further oxidation leads to intermediate **IX**. By rearrangement of the alkyl moiety and subsequent deprotonation products **5″** and **5‴** are obtained. The probability, which of the presented pathways **a)**, **b)**, **c′)** or **c″)** take place, depends strongly on the nature of substituent R^m. However, for substrates bearing a substituent R^p *para* to the alkyl chain, the results indicate that the mechanism proceeds predominantly through spiro intermediate **X**, which can undergo two possible follow-up reactions. If rearrangement **c‴)** takes place, the 6-substituted product **5⁗** is obtained (derivatives **5v** and **5w**). Alternatively, spirolactam **6** can be accessed (pathway **d)**), if substituent R^p enables a stabilization of the intermediate **X** through elimination of a leaving group (derivatives **6x** and **6y**) or through addition of a nucleophile (derivatives **6z** and **6z′**). As a counter reaction, hydrogen is generated at the cathode by deprotonation of HFIP and reduction of the released protons. The mechanism regarding regiochemistry is supported by the literature.[14,16,17,49]

Conclusions

In summary, a new electrocatalytic hypervalent iodine(III)-mediated in-cell synthesis of 1*H*-*N*-aryl-3,4-dihydroquinolin-2-ones has been developed, featuring a low mediator loading and supporting electrolyte concentration, a recyclable solvent, mild reaction conditions, sustainable, inexpensive and readily available electrode materials, as well as a simple galvanostatic set-up. The broad applicability could be demonstrated by synthesizing 23 derivatives in yields up to 96% containing various functional groups such as halide, alkyl, methoxy, ester, cyano, nitro, acyloxy, and acetamido substituents. Additionally, core motifs of various biologically active substances could be accessed by this method. Performing a 10-fold scale-up experiment proved the excellent scalability of the reaction. Furthermore, it was shown that the highly electron-rich *p*-methoxyanilide substrate **4h** could be converted to the corresponding product in 96% yield in a direct electrolysis without using a mediator. Based on the obtained products a reasonable reaction mechanism was proposed.

Experimental Section

General protocol for the electrochemical synthesis of 1*H*-3,4-dihydroquinolin-2-ones 5a–w and spirolactams 6x–z′: A solution of the corresponding *N*-aryl-3-arylpropanamide substrate **4a–z** (0.30 mmol, 1.0 eq.), NBu_4PF_6 (19 mg, 0.01 M), 4-Tol-I (7 mg, 0.03 mmol, 0.1 eq.), and NBu_4OAc (9 mg, 0.03 mmol, 0.1 eq.) in HFIP (5 mL) was stirred (v_{stirr} = 400 rpm) in a temperature adjusted undivided 5 mL Teflon™ screening cell[41] for 30 minutes until the reaction mixture reached a constant temperature of 40 °C. Then, the solution was electrolyzed under constant current conditions (j = 1 mA cm^{-2}; anodic surface: 1.8 cm^2), employing a freshly sanded isostatic graphite anode, and a stainless-steel electrode (undivided set-up) or a stainless-steel wire (quasi-divided set-up) as cathode, until a total applied charge of 2.4 *F* was applied. The solvent was recovered by rotary evaporation (200–90 mbar, 50 °C) and the residue was purified by column chromatography, yielding products **5a–w** or **6x–z′**.

For derivatives, where 5 mol% of the mediator was applied, the following instead of the above stated amounts were used: 4-Tol-I (3 mg, 0.015 mmol, 0.05 eq.), NBu_4OAc (5 mg, 0.015 mmol, 0.05 eq.). For derivatives, where 20 mol% of the mediator was applied, the following instead of the above stated amounts were used: 4-Tol-I (13 mg, 0.06 mmol, 0.2 eq.), NBu_4OAc (18 mg, 0.06 mmol, 0.2 eq.).

For quantification by HPLC, 2-naphthol (1.0 eq.) was added as internal standard to the crude product after having removed HFIP. For quantification by ^{1}H NMR, 1,3,5-trimethoxybenzene (1.0 eq.) was added as internal standard to the crude product after having removed HFIP.

Protocol for the scale-up of the electrochemical synthesis of 5p: A solution of **4p** (0.82 g, 3.0 mmol, 1.0 eq.), NBu_4PF_6 (0.19 g, 0.01 M), 4-Tol-I (0.07 g, 0.3 mmol, 0.1 eq.), and NBu_4OAc (0.09 g, 0.3 mmol, 0.1 eq.) in HFIP (50 mL) was heated in a 60 mL beaker-type glass cell, until the reaction mixture reached 40 °C. Then, the solution was electrolyzed under constant current conditions (j = 1 mA cm^{-2}; anodic surface: 7.2 cm^{-2}), employing a freshly sanded isostatic graphite anode and a spiral-shaped stainless-steel wire as cathode, until a total charge of 2.4 *F* was applied. The solvent was recovered by rotary evaporation (200–90 mbar, 50 °C) and the residue was purified by column chromatography (silica gel, cyclohexane/ ethyl acetate, gradient: 3% to 25% ethyl acetate *v*/*v*), yielding product **5p**.

Supporting Information

The authors have cited additional references within the Supporting Information (Ref. [26, 31–33, 41, 50]).

Acknowledgements

Financial support from the Fonds der Chemischen Industrie (Kekulé Fellowship to J. C. Bieniek) is gratefully acknowledged. This work was supported by the Max Planck Graduate Center with the Johannes Gutenberg University of Mainz (MPGC Fellowship to J. C. Bieniek). We acknowledge the Deutsche Forschungsgemeinschaft (Wa1276/17-2) for financial support. Open Access funding enabled and organized by Projekt DEAL.

Conflict of Interests

The authors declare no conflict of interest.

Data Availability Statement

The data that support the findings of this study are available in the supplementary material of this article.

Keywords: amination · electrochemistry · hypervalent compounds · nitrogen heterocycles · oxidation

[1] I. Tellitu, A. Urrejola, S. Serna, I. Moreno, M. T. Herrero, E. Domínguez, R. SanMartin, A. Correa, *Eur. J. Org. Chem.* **2007**, *2007*, 437.
[2] a) Y. Hayashi, F. Inagaki, C. Mukai, *Org. Lett.* **2011**, *13*, 1778; b) C. Ito, M. Itoigawa, T. Otsuka, H. Tokuda, H. Nishino, H. Furukawa, *J. Nat. Prod.* **2000**, *63*, 1344; c) R. Uchida, R. Imasato, K. Shiomi, H. Tomoda, S. Omura, *Org. Lett.* **2005**, *7*, 5701.
[3] European Medicines Agency, "List of nationally authorised medicinal products. Active substance: carteolol", can be found under http://www.ema.europa.eu/en/documents/psusa/carteolol-list-nationally-authorised-medicinal-products-psusa/00000574/201903_en.pdf, **2019** (accessed 12 August 2023).
[4] a) S. Morita, Y. Irie, Y. Saitoh, H. Kohri, *Biochem. Pharmacol.* **1976**, *25*, 1836; b) S. Lucas, R. Heim, C. Ries, K. E. Schewe, B. Birk, R. W. Hartmann, *J. Med. Chem.* **2008**, *51*, 8077.
[5] D. F. C. Moffat, S. Pintat (Chroma Therapeutics Ltd.), *WO 2008/053158 A1* **2008**.
[6] J. C. Boehm, J. F. Callahan, R. F. Hall, X. Lin, K. L. Widdowson (Smithkline Beecham Corp.), *WO 2004/073628 A2* **2004**.
[7] C. D. Beadle, J. Boot, N. P. Camp, N. Dezutter, J. Findlay, L. Hayhurst, J. J. Masters, R. Penariol, M. W. Walter, *Bioorg. Med. Chem. Lett.* **2005**, *15*, 4432.
[8] Y. Oshiro, Y. Sakurai, S. Sato, N. Kurahashi, T. Tanaka, T. Kikuchi, K. Tottori, Y. Uwahodo, T. Miwa, T. Nishi, *J. Med. Chem.* **2000**, *43*, 177.
[9] a) T. Bifu, P. Biju, T. A. Blizzard, Z. Chen, M. J. Clements, M. Cui, J. L. Frie, W. K. Hagmann, B. Hu, H. Josien, A. G. Nair, C. W. Plummer (Merck Sharp & Dohme Corp.), *WO 2015/176267 A1* **2015**; b) K. Negoro, K. Ohnuki, T. Kurosaki, F. Iwasaki, Y. Yonetoku, K. Tsuchiya, N. Asai, S. Yoshida, T. Soga, D. Suzuki (Astellas Pharma Inc.), *WO 2008/066097 A1* **2008**; c) H.

He, J. Yu, S. Chen (Medshine Discovery Inc.), *CA 3064794 A1* **2018**; d) A. M. Birch, P. W. Kenny, N. G. Oikonomakos, L. Otterbein, P. Schofield, P. R. O. Whittamore, D. P. Whalley, *Bioorg. Med. Chem. Lett.* **2007**, *17*, 394.
[10] T. Nakamura, S. Masuda, A. Fujino (Taisho Pharmaceutical Co. Ltd.), *WO 2010/090347 A1*, **2010**.
[11] D. L. Romero, M. G. Johnson, A. D. Lee, B. Behrouz, E. L. Fritzen Jr. (Vincere Biosciences Inc.), *WO 2021/050992 A1* **2021**.
[12] a) F. Hallé, O. van der Poorten, C. Doebelin, M. Niederst, S. Schneider, M. Schmitt, S. Ballet, F. Bihel, *Tetrahedron Lett.* **2016**, *57*, 1547; b) O. Kitagawa, M. Yoshikawa, H. Tanabe, T. Morita, M. Takahashi, Y. Dobashi, T. Taguchi, *J. Am. Chem. Soc.* **2006**, *128*, 12923; c) L. Porosa, R. D. Viirre, *Tetrahedron Lett.* **2009**, *50*, 4170; d) B. H. Yang, S. L. Buchwald, *Org. Lett.* **1999**, *1*, 35.
[13] a) T. Kukosha, N. Trufilkina, M. Katkevics, *Synlett* **2011**, *17*, 2525; b) N. He, Y. Huo, J. Liu, Y. Huang, S. Zhang, Q. Cai, *Org. Lett.* **2015**, *17*, 374.
[14] Y. Kikugawa, A. Nagashima, T. Sakamoto, E. Miyazawa, M. Shiiya, *J. Org. Chem.* **2003**, *68*, 6739.
[15] S. Reddy Kandimalla, S. Prathima Parvathaneni, G. Sabitha, B. V. Subba Reddy, *Eur. J. Org. Chem.* **2019**, *2019*, 1687.
[16] Q. Ding, H. He, Q. Cai, *Org. Lett.* **2018**, *20*, 4554.
[17] H. Sasa, K. Mori, K. Kikushima, Y. Kita, T. Dohi, *Chem. Pharm. Bull.* **2022**, *70*, 106.
[18] F. V. Singh, S. E. Shetgaonkar, M. Krishnan, T. Wirth, *Chem. Soc. Rev.* **2022**, *51*, 8102.
[19] S. Möhle, M. Zirbes, E. Rodrigo, T. Gieshoff, A. Wiebe, S. R. Waldvogel, *Angew. Chem. Int. Ed.* **2018**, *57*, 6018.
[20] D. Pollok, S. R. Waldvogel, *Chem. Sci.* **2020**, *11*, 12386.
[21] J. L. Röckl, D. Pollok, R. Franke, S. R. Waldvogel, *Acc. Chem. Res.* **2020**, *53*, 45.
[22] J. Seidler, J. Strugatchi, T. Gärtner, S. R. Waldvogel, *MRS Energy Sustainability* **2020**, *7*, e42.
[23] A. Wiebe, T. Gieshoff, S. Möhle, E. Rodrigo, M. Zirbes, S. R. Waldvogel, *Angew. Chem. Int. Ed.* **2018**, *57*, 5594.
[24] T. Dohi, A. Maruyama, Y. Minamitsuji, N. Takenaga, Y. Kita, *Chem. Commun.* **2007**, 1224.
[25] a) M. S. Yusubov, V. V. Zhdankin, *Curr. Org. Synth.* **2012**, *9*, 247; b) Z. Zheng, D. Zhang-Negrerie, Y. Du, K. Zhao, *Sci. China Chem.* **2014**, *57*, 189.
[26] A. Maity, B. L. Frey, N. D. Hoskinson, D. C. Powers, *J. Am. Chem. Soc.* **2020**, *142*, 4990.
[27] B. L. Frey, M. T. Figgins, G. P. Van Trieste III, R. Carmieli, D. C. Powers, *J. Am. Chem. Soc.* **2022**, *144*, 13913.
[28] R. Francke, *Curr. Opin. Electrochem.* **2021**, *28*, 100719.
[29] B. L. Frey, P. Thai, L. Patel, D. C. Powers, *Synthesis* **2023**, *55*, 3019.
[30] a) M. Elsherbini, T. Wirth, *Chem. Eur. J.* **2018**, *24*, 13399; b) C. Chen, X. Wang, T. Yang, *Front. Chem.* **2022**, *10*, 883474; c) R. Francke, *Curr. Opin. Electrochem.* **2019**, *15*, 83.
[31] T. Wirth, *Curr. Opin. Electrochem.* **2021**, *28*, 100701.
[32] T. Broese, R. Francke, *Org. Lett.* **2016**, *18*, 5896.
[33] M. Elsherbini, B. Winterson, H. Alharbi, A. A. Folgueiras-Amador, C. Génot, T. Wirth, *Angew. Chem. Int. Ed.* **2019**, *58*, 9811.
[34] Y. Amano, K. Inoue, S. Nishiyama, *Synlett* **2008**, *1*, 134.
[35] a) Y. Amano, S. Nishiyama, *Tetrahedron Lett.* **2006**, *47*, 6505; b) K. Inoue, Y. Ishikawa, S. Nishiyama, *Org. Lett.* **2010**, *12*, 436.
[36] A. Kehl, V. M. Breising, D. Schollmeyer, S. R. Waldvogel, *Chem. Eur. J.* **2018**, *24*, 17230.
[37] S. Zhang, L. Li, M. Xue, R. Zhang, K. Xu, C. Zeng, *Org. Lett.* **2018**, *20*, 3443.
[38] V. M. Breising, J. M. Kayser, A. Kehl, D. Schollmeyer, J. C. Liermann, S. R. Waldvogel, *Chem. Commun.* **2020**, *56*, 4348.
[39] J. C. Bieniek, M. Grünewald, J. Winter, D. Schollmeyer, S. R. Waldvogel, *Chem. Sci.* **2022**, *13*, 8180.
[40] a) T. Gieshoff, D. Schollmeyer, S. R. Waldvogel, *Angew. Chem. Int. Ed.* **2016**, *55*, 9437; b) A. Kehl, T. Gieshoff, D. Schollmeyer, S. R. Waldvogel, *Chem. Eur. J.* **2018**, *24*, 590; c) A. Kehl, N. Schupp, V. M. Breising, D. Schollmeyer, S. R. Waldvogel, *Chem. Eur. J.* **2020**, *26*, 15847; d) P. Xiong, H.-C. Xu, *Acc. Chem. Res.* **2019**, *52*, 3339.
[41] C. Gütz, B. Klöckner, S. R. Waldvogel, *Org. Process Res. Dev.* **2016**, *20*, 26.
[42] G. Hilt, *ChemElectroChem* **2020**, *7*, 395.
[43] a) B. Elsler, A. Wiebe, D. Schollmeyer, K. M. Dyballa, R. Franke, S. R. Waldvogel, *Chem. Eur. J.* **2015**, *21*, 12321; b) O. Hollóczki, A. Berkessel, J. Mars, M. Mezger, A. Wiebe, S. R. Waldvogel, B. Kirchner, *ACS Catal.* **2017**, *7*, 1846; c) O. Hollóczki, R. Macchieraldo, B. Gleede, S. R. Waldvogel, B. Kirchner, *J. Phys. Chem. Lett.* **2019**, *10*, 1192; d) H. F. Motiwala, A. M. Armaly, J. G. Cacioppo, T. C. Coombs, K. R. K. Koehn, V. M. Norwood, J. Aubé, *Chem. Rev.* **2022**, *122*, 12544.
[44] a) M. Dörr, M. M. Hielscher, J. Proppe, S. R. Waldvogel, *ChemElectroChem* **2021**, *8*, 2621; b) M. Dörr, J. L. Röckl, J. Rein, D. Schollmeyer, S. R. Waldvogel, *Chem. Eur. J.* **2020**, *26*, 10195; c) M. Hielscher, E. K. Oehl, B. Gleede, J. Buchholz, S. R. Waldvogel, *ChemElectroChem* **2021**, *8*, 3904; d) M. M. Hielscher, B. Gleede, S. R. Waldvogel, *Electrochim. Acta* **2021**, *368*, 137420.
[45] T. Gieshoff, A. Kehl, D. Schollmeyer, K. D. Moeller, S. R. Waldvogel, *J. Am. Chem. Soc.* **2017**, *139*, 12317.
[46] Deposition numbers 2299367 (for **6y**), and 2299366 (for **6z'**) contain the supplementary crystallographic data for this paper. These data are provided free of charge by the joint Cambridge Crystallographic Data Center.
[47] a) E. Miyazawa, T. Sakamoto, Y. Kikugawa, *J. Org. Chem.* **2003**, *68*, 5429; b) D. J. Wardrop, M. S. Burge, *J. Org. Chem.* **2005**, *70*, 10271; c) C. Zhang, F. Bu, C. Zeng, D. Wang, L. Lu, H. Zhang, A. Lei, *CCS Chem.* **2022**, *4*, 1199.
[48] a) Y. Ohno, S. Ando, D. Furusho, R. Hifumi, Y. Nagata, I. Tomita, S. Inagi, *Org. Lett.* **2023**, *25*, 3951; b) M. Schubert, K. Wehming, A. Kehl, M. Nieger, G. Schnakenburg, R. Fröhlich, D. Schollmeyer, S. R. Waldvogel, *Eur. J. Org. Chem.* **2016**, *2016*, 60; c) J. Barjau, G. Schnakenburg, S. R. Waldvogel, *Angew. Chem. Int. Ed.* **2011**, *50*, 1415.
[49] D. Liang, W. Yu, N. Nguyen, J. R. Deschamps, G. H. Imler, Y. Li, A. D. MacKerell, C. Jiang, F. Xue, *J. Org. Chem.* **2017**, *82*, 3589.
[50] a) C. Zhao, M. Sun, M. D. Cowart, Y. L. Bennani (Abbott Laboratories), *US 2005/0227953 A1* **2005**; b) D. Pollok, B. Gleede, A. Stenglein, S. R. Waldvogel, *Aldrichimica Acta* **2021**, *54*, 3; c) IKA-Werke GmbH & CO. KG, "Screening System Package (8 Cells)", can be found under http://www.ika.com/en/Products-LabEq/Screening-System-pg913/Screening-System-Package-(8-Cells)-40003642/ (accessed 9 October **2023**); d) J. Hurmalainen, M. A. Land, K. N. Robertson, C. J. Roberts, I. S. Morgan, H. M. Tuononen, J. A. C. Clyburne, *Angew. Chem. Int. Ed.* **2015**, *54*, 7484; e) K. Nozawa-Kumada, S. Saga, Y. Matsuzawa, M. Hayashi, M. Shigeno, Y. Kondo, *Chem. Eur. J.* **2020**, *26*, 4496; f) Merck KGaA, "SynLectro™ Electrolysis Platform", can be found under http://www.sigmaaldrich.com/DE/de/technical-documents/technical-article/chemistry-and-synthesis/organic-reaction-toolbox/synlectro-electrolysis-platform (accessed 27 September 2022); g) J. G. Nathanael, J. M. White, A. Richter, M. R. Nuske, U. Wille, *Org. Biomol. Chem.* **2020**, *18*, 6949; h) K. Okuda, A. C. Seila, S. A. Strobel, *Tetrahedron* **2004**, *60*, 12101; i) P. Natarajan, O. Metin, *Chem. Commun.* **2023**, *59*, 6548; j) P. Yang, X. Wang, Y. Ma, Y. Sun, L. Zhang, J. Yue, K. Fu, J. S. Zhou, B. Tang, *Chem. Commun.* **2020**, *56*, 14083; k) S. Jung, Y. Kawashima, T. Noguchl, N. Imal, *Synthesis* **2019**, *51*, 3683; l) G. M. Sheldrick, *Acta Crystallogr.* **2015**, *C71*, 3; m) L. Wu, Y. Hao, Y. Liu, Q. Wang, *Org. Biomol. Chem.* **2019**, *17*, 6762; n) X. Xie, X. Guo, K. Qiao, L. Shi, *Org. Biomol. Chem.* **2022**, *20*, 8031; o) D. M. Zubrytski, G. Z. Elek, M. Lopp, D. G. Kananovich, *Molecules* **2021**, *26*, 140; p) M. Elsherbini, W. J. Moran, *Org. Biomol. Chem.* **2021**, *19*, 4706; q) G. Laudadio, H. P. L. Gemoets, V. Hessel, T. Noël, *J. Org. Chem.* **2017**, *82*, 11735; r) T. Fuchigami, T. Fujita, *J. Org. Chem.* **1994**, *59*, 7190.

Manuscript received: October 14, 2023
Accepted manuscript online: November 29, 2023
Version of record online: December 13, 2023